

# Mechanical and Thermal Properties of Waterborne Polyurethane Films Modified by $\text{CaCO}_3@ \text{TiO}_2$ Particles with UV Absorption Activity

JIANG Tiechao<sup>1</sup>, FAN Qingqiu<sup>2</sup>, HUANG Chunying<sup>2</sup>, LI Zhen<sup>2</sup>,  
GUO Lijie<sup>2</sup> and ZHOU Bing<sup>2\*</sup>

1. China-Japan Union Hospital of Jilin University, Changchun 130031, P. R. China;

2. College of Chemistry, Jilin University, Changchun 130021, P. R. China

**Abstract**  $\text{CaCO}_3@ \text{TiO}_2$  particles were synthesized through a direct carbonation method, which can be used as the substitutes of  $\text{TiO}_2$  in pigments and coatings. To improve the dispersion in waterborne polyurethane(WPU) suspensions,  $\text{CaCO}_3@ \text{TiO}_2$  particles were modified by stearic acid. SEM tests of the fractured surfaces of the composites films showed that the  $\text{CaCO}_3@ \text{TiO}_2$  particles were well embedded in the WPU matrix. And the mechanical properties, thermal stability and water resistance of the composites films were improved by the introduction of  $\text{CaCO}_3@ \text{TiO}_2$  particles.

**Keywords** Waterborne polyurethane;  $\text{CaCO}_3@ \text{TiO}_2$  particle; *In situ* polymerization

## 1 Introduction

Waterborne polyurethane(WPU) owns excellent features of non-pollution and non-toxicity, and is widely applied in coatings, adhesives, paper, textile, wood or glass fiber, and biodegradable materials<sup>[1–3]</sup> instead of the conventional organic solvent-borne polyurethane(SPU). Compared to SPU, WPU still has some drawbacks such as lower thermal stability, water-resistance, photostability and mechanical strength<sup>[4]</sup>. To improve the performance of WPU, powder composition methods have been used as an effective strategy, such as the introduction of  $\text{CaCO}_3$ <sup>[5]</sup>,  $\text{SiO}_2$ <sup>[6]</sup>,  $\text{TiO}_2$ <sup>[7]</sup>, clay<sup>[8]</sup>, ZnO<sup>[9]</sup>, Ag<sup>[10]</sup>, graphene<sup>[11,12]</sup> in WPU dispersions<sup>[13]</sup>.

Yao *et al.*<sup>[5]</sup> had prepared stable WPU/ $\text{CaCO}_3$  hybrids with good dispersion of  $\text{CaCO}_3$  by gas-diffusion mineralization method, and the thermal stability, water penetration and chemical resistance of the hybrid films were improved. Che *et al.*<sup>[7]</sup> obtained Nano- $\text{TiO}_2$ /PU emulsions *via in situ* RAFT(reversible addition-fragmentation chain transfer) polymerization of HEA-end capped PUM emulsions(HEA=hydroxyethyl acrylate). The tensile strengths of the composite films were significantly enhanced and the nano- $\text{TiO}_2$ /PU emulsions were stable enough not to precipitate in at least three months<sup>[6]</sup>. Therefore, the interaction between the fillers and PU chains should be considered before the composition process<sup>[14]</sup>.

We had reported two routes to prepare WPU/ $\text{CaCO}_3$  and WPU/ $\text{SiO}_2$  composites films, which only focus on the basic synthesis method, not the specific properties derived from the fillers<sup>[15]</sup>.

Core-shell structured  $\text{CaCO}_3@ \text{TiO}_2$  particles could be

considered as the potential substitute of commercial  $\text{TiO}_2$ , for its outer layer was composed of  $\text{TiO}_2$  nano-sheets to exhibit most properties of  $\text{TiO}_2$ , which leads to lower the consumption of  $\text{TiO}_2$ <sup>[16]</sup>. Various methods have been reported for the synthesis of  $\text{CaCO}_3@ \text{TiO}_2$  composite, including template method<sup>[12]</sup>, liquid deposition method<sup>[13]</sup>, sol-precipitation routes<sup>[14,15]</sup>, and mechanochemical method<sup>[14]</sup>.

In this study,  $\text{CaCO}_3@ \text{TiO}_2$  particles were prepared by bubbling  $\text{CO}_2$  gas into  $\text{Ca}(\text{OH})_2$ - $\text{TiO}_2$  slurry as reported before<sup>[17]</sup>. WPU/ $\text{CaCO}_3@ \text{TiO}_2$  composites were obtained by *in situ* polymerization method<sup>[18,19]</sup>. The properties of WPU/ $\text{CaCO}_3@ \text{TiO}_2$  composites films were studied by scanning electron microscopy(SEM), thermogravimetric analysis(TGA), UV-Visible spectrometry, mechanical testing and water swelling testing<sup>[20]</sup>. WPU/ $\text{CaCO}_3@ \text{TiO}_2$  composites can be potentially applied in coatings and textiles fields<sup>[21]</sup>.

## 2 Experimental

### 2.1 Materials

CaO was supplied by Menghe Chemical Reagent Factory. Rutile-type  $\text{TiO}_2$  treated by silica and alumina was supplied by Panzhihua Iron and Steel Group. polypropylene glycol (PPG, Yantai Wanhua Polyurethanes Co., Ltd.) was dried for 12 h at 80 °C under vacuum to eliminate the inner moisture before use. 2,2-Bishydroxymethyl propionic acid(DMPA), which was purchased from Alfa Aesar, America was dehydrated at 80 °C under vacuum for 24 h. Toluene diisocyanate (TDI), stearic acid(SA), dibutyltin dilaurate(DBTDL), trimethylamine(TEA) and acetone were all of analytical grade.

\*Corresponding author. E-mail: zhoubing@jlu.edu.cn

Received March 9, 2017; accepted May 19, 2017.

Supported by the National Natural Science Foundation of China(No.21671078).

© Jilin University, The Editorial Department of Chemical Research in Chinese Universities and Springer-Verlag GmbH

## 2.2 Preparation of CaCO<sub>3</sub>@TiO<sub>2</sub> Particles

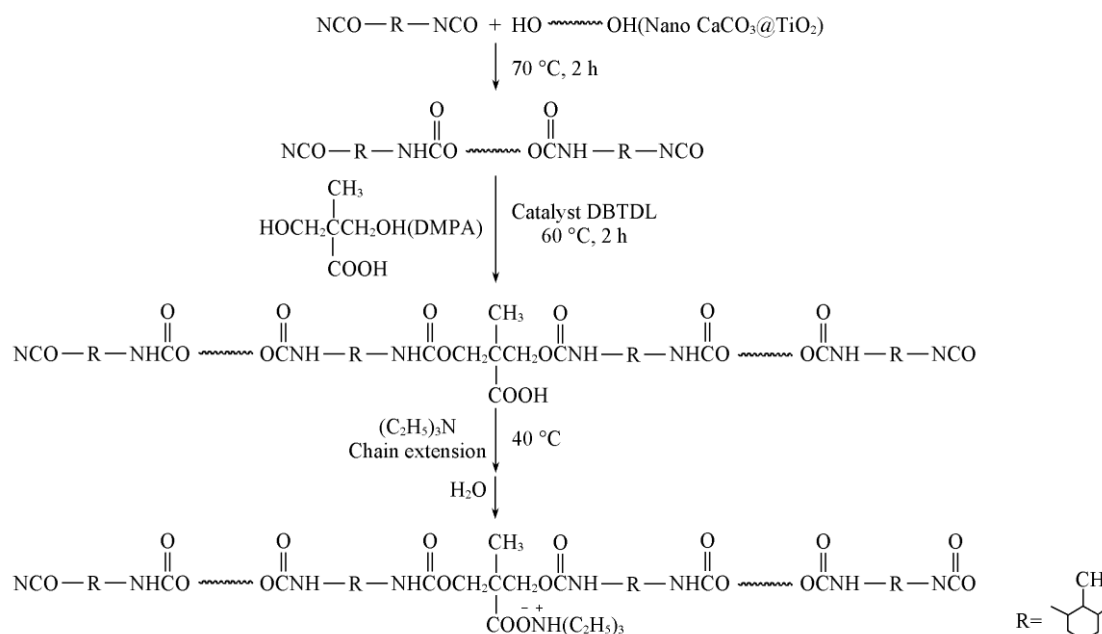
Firstly, 60 g of CaO was put in distilled water to form 10% (mass fraction) Ca(OH)<sub>2</sub> slurry. Then, a certain amount of commercial TiO<sub>2</sub> powder was added to the above Ca(OH)<sub>2</sub> slurry in a vessel, and homogenized by ultrasonic vibration for 30 min. The carbonization reaction monitored by pH value of the slurry was carried out under 40 °C in water bath. The gas mixture (CO<sub>2</sub>/N<sub>2</sub>, volume ratio 1:2) was bubbled into the suspension through a quartz tube at a flow rate of 1 L/min until the pH value of the slurry reached 7. The precipitates were separated from the liquor by filtration and washed five times with distilled water, then dried at 120 °C for 12 h in an oven.

## 2.3 Surface Modification of CaCO<sub>3</sub>@TiO<sub>2</sub> Particles

Firstly, 8 g of CaCO<sub>3</sub>@TiO<sub>2</sub> particles were dispersed in water with mechanical stirring at 90 °C. Then, 0.2 g of SA and 0.014 g of NaOH dissolved in 10 mL of ethanol were added to the above-mentioned solution under continuous stirring. The final products (SA-CaCO<sub>3</sub>@TiO<sub>2</sub>) were obtained by filtration, washed and dried at 120 °C for 24 h.

## 2.4 Synthesis of WPU/CaCO<sub>3</sub>@TiO<sub>2</sub> Composites Films

A 500 mL round-bottom, 4-necked glass flask with a mechanical stirrer, a nitrogen inlet and a condenser was used as the reactor for the preparation of WPU/CaCO<sub>3</sub>@TiO<sub>2</sub> composites. The synthesis procedures of the composite are shown as follows: 20 mL of acetone mixed with 0.73 g of CaCO<sub>3</sub>@TiO<sub>2</sub> particles were added to 22.2 g of PPG in the flask, which was kept at room temperature for 10 min under stirring. Excess TDI was charged into the flask, and the suspension was heated at 70 °C for 2 h. Then certain amounts of DMPA and DBTDL were added and the mixture was heated at 60 °C for another 2 h. During the above process, extra acetone was used to adjust the viscosity of the WPU prepolymers. When the reaction mixture was cooled to 40 °C, TEA was added and agitated for 30 min to neutralize the carboxylic groups of DMPA. Finally, an aqueous emulsion was obtained by adding 120 mL of distilled water to the mixture with vigorous stirring. The WPU/CaCO<sub>3</sub>@TiO<sub>2</sub> composites film was prepared by casting the emulsion onto Teflon mold under heating in a vacuum oven at 60 °C for 24 h. The process is shown in Scheme 1.



Scheme 1 Flowchart of the preparation of WPU/CaCO<sub>3</sub>@TiO<sub>2</sub> composites

## 2.5 Characterization and Property Measurements

Fourier transform infrared (FTIR) spectra of CaCO<sub>3</sub>@TiO<sub>2</sub> particles and WPU/CaCO<sub>3</sub>@TiO<sub>2</sub> composites were identified in the wavenumber range of 4000–400 cm<sup>-1</sup> at a resolution of 4 cm<sup>-1</sup> using a JIR-5500 (JEOL) spectrophotometer at room temperature. UV-visible transmission spectra of particles were obtained on a UV-2550 (Shimadzu) UV-visible spectrometer. X-ray powder diffraction (XRD) data of CaCO<sub>3</sub>@TiO<sub>2</sub> particles and composites films were collected on a Rigaku 2400 X-ray diffractometer (Cu K $\alpha$  radiation,  $\lambda=0.15418$  nm). Thermogra-

vimetric analysis (TGA) was carried out on a DTG-60H (Shimadzu) analyzer at a heating rate of 20 °C/min under nitrogen atmosphere. Scanning electron microscope (SEM, XL30 ESEM-FEG) was used to observe the dispersion of CaCO<sub>3</sub>@TiO<sub>2</sub> powders in WPU films. Mechanical properties of the casting films were measured at 25 °C by a universal mechanical testing machine (Shimadzu AGS-J) in accordance with GB1040-79 at a crosshead speed of 50 mm/min. For each data point, five specimens were tested and the average value was reported. Water swelling values of the hybrid films were collected as follows: pre-weighed dry samples (20 mm×20 mm) were totally immersed in distilled water at 25 °C for 12 h.

Water swelling was expressed as the mass percentage of water in the swollen sample and calculated by the following equation:

$$\text{Swelling}(\%) = [(m_2 - m_1) / m_1] \times 100\% \quad (1)$$

where  $m_1$  and  $m_2$  are the mass of the original dry sample and the swollen sample, respectively.

### 3 Results and Discussion

#### 3.1 Morphology Characterization

Fig.1 shows the SEM images of the  $\text{CaCO}_3$  (prepared under the same conditions as  $\text{CaCO}_3@TiO_2$ ), commercial  $TiO_2$ ,  $\text{CaCO}_3@TiO_2$  and the fractured surface of WPU/ $\text{CaCO}_3@TiO_2$  composites films. From Fig.1(A) we can observe that the  $\text{CaCO}_3$  particle is spindle-shaped, and its diameter and length are about 200 and 600 nm, respectively. Fig.1(B) shows that commercial  $TiO_2$  particle was spherical with an average diameter of about 200 nm. As shown in Fig.1(C), the as-synthesized core-shell structured  $\text{CaCO}_3@TiO_2$  particles are also spindle-shaped, but the size become bigger and the particles' surface grow coarser after being coated by  $TiO_2$

nano-sheets. In addition, no extra  $TiO_2$  particles can be observed, indicating that the commercial  $TiO_2$  particles were converted into slice layer on  $\text{CaCO}_3$  particles surface, attributed to the disaggregation of original  $TiO_2$  particles under alkaline conditions during mechanical stirring. The combination of  $\text{CaCO}_3$  and  $TiO_2$  particles was chiefly physical adsorption of electrostatic attraction<sup>[18]</sup>. In Fig.1(D), the fractured surface of pristine WPU showed a smooth surface, different from that of the WPU/ $\text{CaCO}_3@TiO_2$  composites films. In Fig.1(E), the particles aggregates obviously because of their high surface energy and low surface reactive capacity. In contrast, a homogeneous distribution of SA- $\text{CaCO}_3@TiO_2$  in the WPU matrix is observed without large aggregates or agglomeration [Fig.1(F)], which demonstrates that the particles were well adhered to the WPU matrix. Therefore, the adhesion between the particles and WPU matrix became better due to the active surface originated from the treatment by SA<sup>[21]</sup>. Such a good distribution of the additives in the WPU matrix could play an important role in improving the thermal and mechanical properties of the resulting composite films<sup>[15]</sup>.

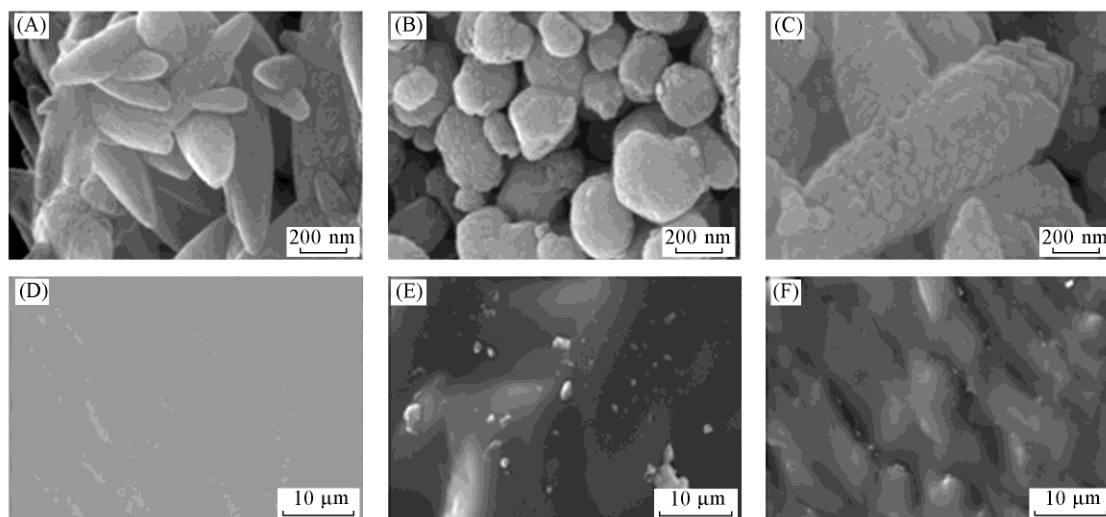


**Fig.1** SEM images of  $\text{CaCO}_3$ (A), commercial  $TiO_2$ (B),  $\text{CaCO}_3@TiO_2$ (C), pure WPU(D), WPU/ $\text{CaCO}_3@TiO_2$ (E) and WPU/SA- $\text{CaCO}_3@TiO_2$ (F)

#### 3.2 XRD Analysis

Fig.2 shows the XRD patterns of the  $\text{CaCO}_3$ ,  $TiO_2$ ,  $\text{CaCO}_3@TiO_2$  particles, WPU and WPU/ $\text{CaCO}_3@TiO_2$  composites. The diffraction peaks of pure calcite phase  $\text{CaCO}_3$

[Fig.2(A) pattern *a*, JCPDS No. 47-1743] is presented in the patterns of those samples except  $TiO_2$  and WPU. And the diffraction peaks of  $TiO_2$  correspond with those of the rutile phase<sup>[19]</sup> [Fig.2(A) pattern *b*, JCPDS No. 4-0551]. From Fig.2 pattern *c*, it can be seen clearly that this composites is

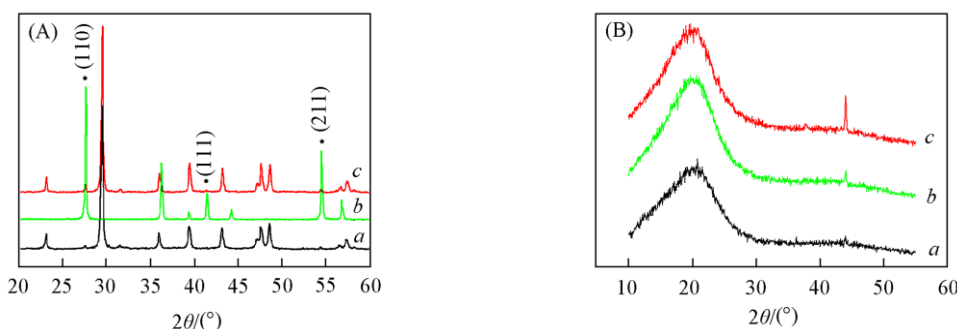


**Fig.2** XRD patterns of  $\text{CaCO}_3$ (a),  $TiO_2$ (b),  $\text{CaCO}_3@TiO_2$ (c)(A) and pure WPU(a), WPU/ $\text{CaCO}_3@TiO_2$ (b) and WPU/SA- $\text{CaCO}_3@TiO_2$ (c)(B)

composed of  $\text{CaCO}_3$  and  $\text{TiO}_2$ . As shown in Fig.2(B), the XRD pattern indicates that the pure WPU is amorphous, and the  $\text{WPU}/\text{CaCO}_3@/\text{TiO}_2$  or  $\text{WPU}/\text{SA}-\text{CaCO}_3@/\text{TiO}_2$  has similar diffraction peaks, which proves that there is no change on the structure of WPU matrix by the addition of particles. However, there is a weak peak at around  $2\theta$  of  $44^\circ$  corresponding to the characteristic peaks of  $\text{CaCO}_3$ , which proves that the particles has successfully embedded into the WPU solid films.

### 3.3 FTIR Analysis

Fig.3(A) shows the FTIR spectra of  $\text{CaCO}_3@/\text{TiO}_2$ ,  $\text{CaCO}_3@/\text{TiO}_2$  modified by SA and the pure SA, respectively. In Fig.3(A) spectrum *b*, new absorption bands belonged to SA is presented at  $2920$  and  $2860\text{ cm}^{-1}$  (stretching vibration of the  $-\text{CH}_2$ )<sup>[20]</sup>, which suggests that SA molecular has grafted on the surface of  $\text{CaCO}_3@/\text{TiO}_2$  successfully, although the powder sample was extracted by alcohol several times. Fig.3(B) shows the representative FTIR spectra of WPU,  $\text{WPU}/\text{CaCO}_3@/\text{TiO}_2$  and  $\text{WPU}/\text{SA}-\text{CaCO}_3@/\text{TiO}_2$ , respectively. All the samples exhibited the characteristic peaks of WPU<sup>[2,5,7]</sup>, proving that the main structure of the  $\text{WPU}/\text{CaCO}_3@/\text{TiO}_2$  composites remains the same as that of the pure WPU.

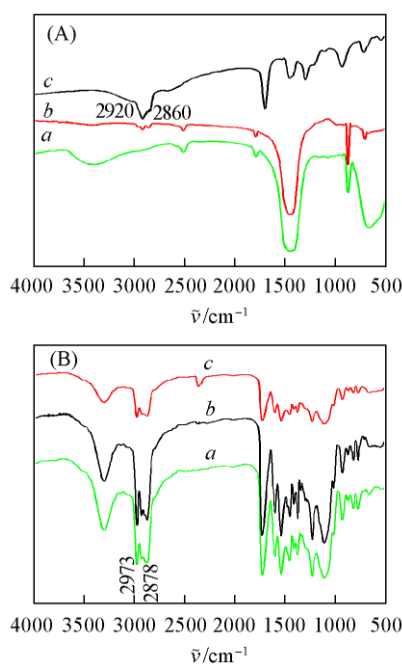


**Fig.3** FTIR spectra of  $\text{CaCO}_3@/\text{TiO}_2$ (*a*),  $\text{SA}-\text{CaCO}_3@/\text{TiO}_2$ (*b*),  $\text{SA}$ (*c*)(A) and pure  $\text{WPU}$ (*a*),  $\text{WPU}/\text{CaCO}_3@/\text{TiO}_2$ (*b*) and  $\text{WPU}/\text{SA}-\text{CaCO}_3@/\text{TiO}_2$ (*c*)(B)

### 3.4 UV-visible Diffuse Reflectance Spectra Analysis

From Fig.4, it is found that the UV-Vis diffuse reflectance spectra(DRS) of both commercial  $\text{TiO}_2$  and  $\text{CaCO}_3@/\text{TiO}_2$  present the absorption regions from  $200\text{ nm}$  to  $400\text{ nm}$ , but the intensity of  $\text{CaCO}_3@/\text{TiO}_2$  composite decreases because  $\text{CaCO}_3$  as the template of  $\text{TiO}_2$  layers has no contribution on UV absorption. However, such materials with perfect UV absorption

ability can also prevent the light degradation of polymer films<sup>[19]</sup>.

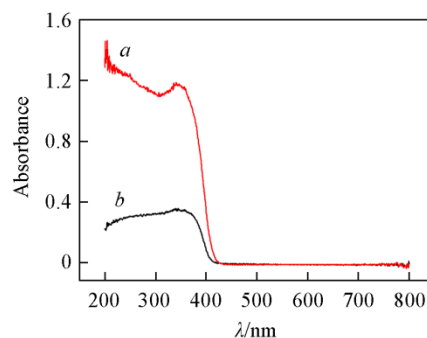


**Fig.4** UV-Vis diffuse reflectance spectra of commercial  $\text{TiO}_2$ (*a*) and  $\text{CaCO}_3@/\text{TiO}_2$ (*b*)

### 3.5 Thermal Properties

Fig.5 exhibits the thermal decomposition behaviors of the pure WPU and  $\text{WPU}/\text{CaCO}_3@/\text{TiO}_2$  composites under a nitrogen atmosphere. Two stages of decomposition appear at the TGA curves of all samples. The first mass loss step is the decomposition of the soft segment of WPU and the second stage is of the hard segment of WPU<sup>[4,20]</sup>. In Fig.5 curve *b*, the decomposition temperature of the hard segment increases by  $11\text{ }^\circ\text{C}$  due to the incorporation of unmodified particles, but it has no effect on the decomposition stage of soft segment. While the adding of  $\text{SA}-\text{CaCO}_3@/\text{TiO}_2$  altered the decomposition temperature remarkably, the decomposition temperature of hard segment is changed from  $264\text{ }^\circ\text{C}$  of pure WPU to  $296\text{ }^\circ\text{C}$ . It could be explained that the formation of the physical crosslinking between the particles and WPU matrix could limit the movement of the WPU chains due to the good dispersion of the particles in the WPU matrix.

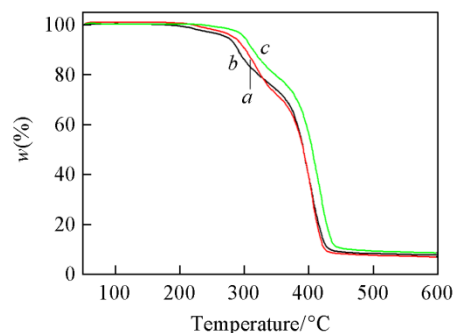


**Fig.5** TGA curves of pure  $\text{WPU}$ (*a*),  $\text{WPU}/\text{CaCO}_3@/\text{TiO}_2$ (*b*) and  $\text{WPU}/\text{SA}-\text{CaCO}_3@/\text{TiO}_2$ (*c*)

### 3.6 Tensile Properties

The stress-strain curves of  $\text{WPU}/\text{CaCO}_3@/\text{TiO}_2$  composites are shown in Fig.6. It is found that pure WPU displays a nonlinear elastic behavior and possesses a low tensile strength of  $4.5\text{ MPa}$  and a high elongation at break of  $1659\%$  because of its amorphous nature. The tensile strength of  $\text{WPU}/\text{CaCO}_3@/\text{TiO}_2$  composites increases to  $6.67\text{ MPa}$ , while that of  $\text{WPU}/\text{SA}-\text{CaCO}_3@/\text{TiO}_2$  composites increases to  $7.98\text{ MPa}$ . The introduction of  $\text{CaCO}_3@/\text{TiO}_2$  particles also improves the tensile modulus of the composites due to the enhancement of

the interfacial interaction between particles and WPU<sup>[21]</sup>. But the elongation at break of the WPU/SA-CaCO<sub>3</sub>@TiO<sub>2</sub> decreases to 813%. This is primarily because of the enhance of interfacial strength between WPU matrix and particles from possible physical cross-linking effect<sup>[5-9]</sup>.

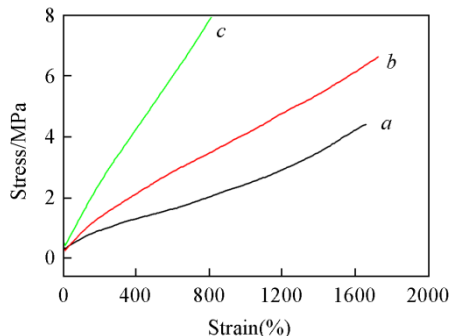


**Fig.6** Stress-strain curves of WPU(a), WPU/CaCO<sub>3</sub>@TiO<sub>2</sub>(b) and WPU/SA-CaCO<sub>3</sub>@TiO<sub>2</sub>(c)

### 3.7 Water Resistance

In Table 1, the water swelling of WPU/CaCO<sub>3</sub>@TiO<sub>2</sub> composites film is lower than that of pure WPU (from 68.65% to 26.24%), and for WPU/SA-CaCO<sub>3</sub>/TiO<sub>2</sub> composites film, it decreases to 13.11%. One possible reason is that the chain densification of WPU is improved by the addition of particles<sup>[4]</sup>, the other reason may be that a mesh structure is formed between the additives and WPU matrix which prevents the water entrance<sup>[17]</sup>. The water resistance of the composites films was modified remarkably, which indicates that such materials could be applied as functional films in the coatings and textiles fields.

**Table 1** Water swelling behavior of WPU/CaCO<sub>3</sub>@TiO<sub>2</sub> composites

Sample	$m_1/g$	$m_2/g$	Water swelling(%)
WPU	0.0992	0.1673	68.65
WPU/CaCO <sub>3</sub> @TiO <sub>2</sub>	0.1246	0.1573	26.24
WPU/SA-CaCO <sub>3</sub> @TiO <sub>2</sub>	0.1289	0.1458	13.11

## 4 Conclusions

In this work, CaCO<sub>3</sub>@TiO<sub>2</sub> particles have been successfully prepared by a facile carbonation method. The results of SEM demonstrated that the CaCO<sub>3</sub> particles were

coated by TiO<sub>2</sub> nano-sheets, and the CaCO<sub>3</sub>@TiO<sub>2</sub> presented specific characters of both CaCO<sub>3</sub> and TiO<sub>2</sub>. While the composite tended to aggregate together since the CaCO<sub>3</sub>@TiO<sub>2</sub> had large specific surface and high surface tension. SEM images proved that the CaCO<sub>3</sub>@TiO<sub>2</sub> modified by SA had a good dispersion in WPU. The thermal stability and mechanical properties could be effectively improved by the addition of SA-CaCO<sub>3</sub>@TiO<sub>2</sub> into WPU matrix, which means this novel materials may be applied in coatings and textiles fields.

## References

- [1] Garcia P. V., Martín M. J. M., *Prog. Org. Coat.*, **2011**, *71*, 136
- [2] Gao Z. Z., Peng J., Zhong T. H., *Carbohydrate Polymers*, **2012**, *87*, 2068
- [3] Wu G. M., Chen J., Huo S. P., *Carbohydrate Polymers*, **2014**, *105*, 207
- [4] Qu Y. C., Jing L. Q., Wang W. X., Fu H. G., Liu Y., *Chem. Res. Chinese Universities*, **2011**, *27*(1), 1
- [5] Yao L., Yang J., Song R., *Mater. Chem. Phys.*, **2011**, *129*, 523
- [6] Yeh J. M., Yao C. T., Hsieh C. F., Yang H. C., Wu C. P., *Eur. Polym. J.*, **2008**, *44*(9), 2777
- [7] Che X. C., Jin Y. Z., Li Y. S., *Prog. Org. Coat.*, **2010**, *69*, 534
- [8] Hson T. L., Li H. L., *Macromolecules*, **2006**, *39*, 6133
- [9] Ma X. Y., Zhang W. D., *Polym. Degrad. Stab.*, **2009**, *94*, 1103
- [10] Shan H. H., Hsiang J. T., Lin Y. C., *Biomaterials*, **2010**, *31*, 6796
- [11] Wang X., Xing W. Y., Song L., *Surface & Coatings Technology*, **2012**, *206*, 78
- [12] Choi S. H., Kim D. H., Raghu A. V., Reddy K. R., Lee H., Yoon K. S., *J. Macromol. Sci. Part B: Physics*, **2012**, *51*(1), 37
- [13] Ghorbel K., Litaïem H., Ktari L., Garcia-Granda S., Dammak M., *Chem. Res. Chinese Universities*, **2016**, *32*(6), 902
- [14] Zhang N., Liu S., Xu Y. J., *J. Phys. Chem. C*, **2011**, *115*, 9136
- [15] Gao X. Y., Zhou B., *Colloid Surf., A: Physicochem. Eng. Aspects*, **2011**, *377*, 312
- [16] Zhang X. N., Zhong X. W., Yang Z., Song J. P., Lu H. Y., *Chem. Res. Chinese Universities*, **2016**, *32*(6), 1016
- [17] Sun D. D., Cao Y. Y., Xu Y. Y., Zhang G. Y., Sun Y. Q., *Chem. Res. Chinese Universities*, **2016**, *32*(6), 882
- [18] Li J. H., Hong R. Y., *Prog. Org. Coat.*, **2009**, *64*, 504
- [19] Kuan H. C., Ma M. C. C., Chang W. P., Yuen S. M., Wu H. H., Lee T. M., *Compo. Sci. Technol.*, **2005**, *65*(1), 1703
- [20] Zhang S. W., Liu R., *Prog. Org. Coat.*, **2011**, *70*, 1
- [21] Bala H., Yu Y. H., *Mater. Lett.*, **2008**, *62*, 2070